

Smart virtual rotor for frequency stability enhancement considering inverter-based renewable energy sources

Herlambang Setiadi¹, Baity Nuris Syifa², Muhammad Abdillah³, Yusrizal Afif⁴

¹Electrical Engineering Study Program, School of Electrical Engineering, Telkom University, Bandung, Indonesia

²School of Electrical Engineering and Computer Science, Faculty of Engineering, Architecture and Information Technology, University of Queensland, Brisbane, Australia

³Department of Electrical Engineering, Faculty of Industrial Technology, Universitas Pertamina, Jakarta, Indonesia

⁴Department of Engineering, Faculty of Advanced Technology and Multidiscipline, Universitas Airlangga, Surabaya, Indonesia

Article Info

Article history:

Received Dec 5, 2024

Revised Jul 26, 2025

Accepted Sep 11, 2025

Keywords:

Bat Algorithm

Clean energy technology

Extreme learning machine

Renewable energy

Virtual rotor controller

ABSTRACT

This paper proposes a novel smart virtual rotor controller (VRC) that combines the Bat Algorithm (BA) with extreme learning machine (ELM) to enhance frequency stability in power systems. To reflect the impact of renewable integration, inverter-based power plants are incorporated to simulate high levels of penetration from power-electronics-based generation. The proposed method first tunes the virtual rotor parameters (virtual inertia and damping control) using BA under varying operating conditions. These parameters are then trained with ELM to enable adaptive control across different scenarios. Time-domain simulations demonstrate that the proposed approach outperforms existing methods in terms of frequency nadir and settling time, while also achieving a significant reduction in execution time, requiring only 0.0033 seconds.

This is an open access article under the [CC BY-SA](https://creativecommons.org/licenses/by-sa/4.0/) license.



Corresponding Author:

Herlambang Setiadi

Electrical Engineering Study Program, School of Electrical Engineering, Telkom University

Sukapura, Dayeuhkolot, Bandung, West Java 40257, Indonesia

Email: herlambangsetiadi@telkomuniversity.ac.id

1. INTRODUCTION

The growing integration of renewable energy sources (RESs) is shifting the generation paradigm from conventional fossil-fuel-based plants toward renewable-based generation [1], [2]. Since RESs interface with the grid through power electronic converters [3], [4], they inherently lack inertial response. Consequently, higher penetration of power-electronics-based RESs reduces total system inertia and increases the rate of change of frequency (RoCoF) during disturbances. Elevated RoCoF not only heightens the risk of frequency instability but also undermines overall system reliability.

Research by Arora *et al.* [5], investigate the impact of adding inverter-based power plants on interconnected power systems. It is reported that adding an inverter-based power plant will bring new challenges to frequency stability. Integrating RESs also increases the non-linearity of the power system as reported in [6]. It is noticeable that if the system's non-linearity is increasing the possibility of the system being unstable is higher. This makes the frequency stability of the system more vulnerable to disturbance. The impact of power electronics-based RESs on frequency stability is reported in [7]. From [7], it is noticeable that adding inverter-based RESs could increase the frequency nadir of the system. In addition, it is reported that to handle the high penetration of RESs, traditional load frequency control is not sufficient.

Another issue from power electronics-based RESs especially photovoltaics (PV) and wind is the intermittent power [8], [9]. The intermittent power of PV and wind happens due to the uncertain power source of the PV and wind [10], [11]. To handle the uncertainty output of PV and wind energy storage is

essential [12], [13]. Research efforts in [14], [15] investigate the influence of energy storage to handle the uncertainty of inverter-based RESs. It is reported that by adding energy storage the stability of the power system can be enhanced. Although energy storage can be the solution to handle the uncertain power output of RESs, the inertia-less characteristic of RESs can not be handled only by original energy storage [16], [17]. Hence, an additional controller that can emulate inertia to the system without adding more conventional power plants is important.

The controller that can emulate inertia or mimic the behavior of a conventional power plant is called a virtual inertia/virtual rotor [18]. It is reported that by adding virtual inertia/virtual rotor to the energy storage the frequency stability of the power system can be enhanced [19]. It is also reported that although the system has low inertia, by adding virtual inertia/virtual rotor controller (VRC) the frequency nadir of the system can be enhanced (far from nadir). The problem with a VRC is how to design the controller optimally, especially if the system is experiencing uncertain conditions from RESs and the load.

The application of manta ray foraging optimization (MRFO) for the development of virtual inertia controllers has been presented in [20], where an islanded microgrid was employed as the benchmark system with RESs integrated into the study. Results demonstrated that MRFO provides an effective means for achieving optimal controller design. Likewise, the utilization of the bacteria foraging optimization algorithm (BFOA) was reported in [21], showing that embedding a virtual inertia controller within inverter-based distributed generation enhances the frequency's dynamic response. Despite their effectiveness, metaheuristic techniques such as MRFO and BFOA encounter significant challenges when system operating conditions vary, as parameter tuning must be continuously adjusted to maintain performance. This limitation highlights the necessity for an adaptive VRC capable of responding to diverse and changing operational environments.

To address this issue, this paper introduces an intelligent VRC that integrates the Bat Algorithm (BA) with the extreme learning machine (ELM). The BA is employed to achieve optimal parameter selection, while the ELM provides adaptability across different operating conditions. Together, this hybrid approach ensures both optimal tuning and real-time adaptability, offering a more robust solution compared to conventional metaheuristic-based designs.

2. METHOD

2.1. Virtual rotor controller

VRC is based on applying the swing equation to inverter-based power plants, enabling inverters without physical inertia to emulate the inertial characteristics of synchronous generators [22]. The term *virtual rotor* reflects the ability to reproduce generator-like rotor dynamics without a rotating mass. Such controllers regulate the amount of additional inertial power supplied to the system [23].

Figure 1 illustrates the dynamic structure of the VRC applied in frequency stability analysis. The VRC incorporates inverter-based energy storage, which is typically represented using a first-order model. To ensure operational safety, a limiter is included to restrict the maximum power output from the storage unit. The virtual rotor itself is generally implemented through a proportional–derivative (PD) controller, where the proportional component emulates virtual damping and the derivative component emulates virtual inertia [24].

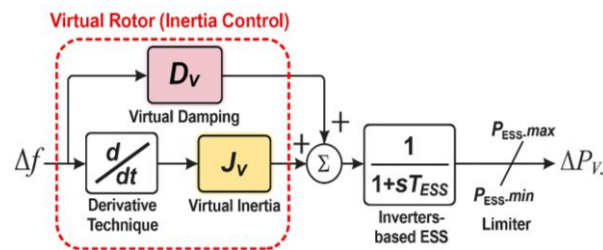


Figure 1. Virtual rotor block diagram

The virtual inertia is calculated using a derivative-based method that relies on the rate of change of frequency (df/dt or RoCoF), enabling adaptive adjustment of active power injection. Through this mechanism, virtual inertia reduces frequency overshoot, while virtual damping enhances the rate of frequency recovery following disturbances or high renewable energy integration [25]. The damping effect is analogous to the function of damper windings in synchronous machines, effectively suppressing oscillations after a frequency event. The governing dynamic equation of the virtual rotor can be expressed as (1) [26]:

$$\Delta P_{VJ} = \frac{I_{VI} S + D_{VI}}{1 + s T_{BES}} (\Delta f) \quad (1)$$

2.2. Bat Algorithm

The BA, proposed by Xin-She Yang in 2010 [27], is a nature-inspired metaheuristic optimization technique modelled on the echolocation behavior of bats. Unlike most mammals, bats are capable of flight and rely on echolocation—a biological sonar—to navigate, detect prey, and avoid obstacles in darkness. They emit ultrasonic pulses and interpret the returning echoes to sense their environment. Depending on the species, these signals may vary in form: some predominantly use short frequency-modulated pulses, while others rely on constant-frequency emissions. The signal bandwidth can also differ among species and often exhibits harmonic components. This echolocation capability enables bats to forage effectively at night without collisions. The design of the BA is guided by three idealized behavioral rules [28]:

- Bats employ echolocation to estimate distance and distinguish prey from obstacles, even in darkness.
- They search for food by flying randomly with velocity v_i at position x_i , using a fixed frequency f_i , wavelength λ_i and loudness A_i .
- Loudness A_i decreases dynamically, typically modeled from an initial maximum value A_0 to a minimum constant value A_{min} .
- The noise level can be varied in various ways, it can be assumed that the noise level varies from a maximum (positive) (A_0) to a minimum constant value (A_{min}).

The BA begins by initializing a population of bats, each defined by an initial position (solution), pulse rate, and frequency. In each iteration, bats update their positions toward the global best solution. When a bat discovers a better solution, its pulse rate and loudness are adjusted accordingly. Throughout the process, the best solution is continuously updated until the stopping criterion is satisfied, at which point the optimal solution is obtained. The pseudocode of BA is described below:

```

Objective function  $f(x)$ , with  $x=(x_1, \dots, x_d)^T$ 
Initialization of Bat algorithm population  $x_i$ ,  $i=1, 2, \dots, n$ , and  $v_i$  randomly
Define the frequency  $f_i$  based on  $x_i$ 
Initialization of the pulse  $r_i$  and loudness  $A_i$  randomly
While ( $t < \text{Maximum iteration}$ )
  Find a new solution by adjusting the frequency
  Update the velocity and the location/ solution using,
       $f_i = f_{min} + (f_{max} - f_{min})\beta$ 
       $v_i^{t+1} = v_i^t + (x_i^t - x^*)f_i$ 
       $x_i^{t+1} = x_i^t + v_i^t$ 

  If  $\text{rand} > r_i$ 
    Choose the best solution
    Use the local solution from the best-chosen solution
  end if
  if ( $\text{rand} < A_i$ ) && ( $f(x_i) < f(x^*)$ )
    Get the new solution
    Increase the  $r_i$  value and decrease the  $A_i$  value
  end if
end while

```

with a $\beta \in [0,1]$ is a random number with uniform distribution. While x^* is the optimal location of the whole solution.

2.3. Extreme learning machine

The ELM, introduced by Guang-Bin Huang, is a learning framework derived from artificial neural networks. It is structured as a feedforward neural network with a single hidden layer, commonly referred to as a single hidden layer feedforward neural network (SLFN). ELM was specifically developed to address the drawbacks of conventional feedforward networks, most notably their slow training process. The inefficiency of traditional approaches can largely be attributed to two main factors [29]: i) reliance on slow gradient-based learning algorithms during training and ii) iterative adjustment of network parameters.

Conventional methods such as backpropagation (BP) and Levenberg–Marquardt (LM) determine parameters—specifically input weights and hidden biases—iteratively, which increases training time and often leads to convergence at local minima. In contrast, ELM assigns input weights and hidden biases randomly, enabling faster training while maintaining strong generalization performance. The structure of the ELM is illustrated in Figure 2.

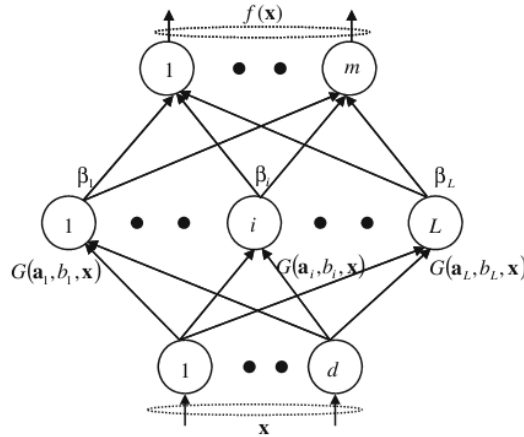


Figure 2. ELM structure

For example, given N distinct training samples (x_i, t_i) $(x_i, t_i) \in R^d \times R^m$, the standard SLFN with L hidden nodes can be mathematically represented as in (2) [30].

$$\text{the } \sum_{i=1}^L \beta_i g_i(x_j) = \sum_{i=1}^L \beta_i G(a_i, b_i, x_j) = o_j, j = 1, \dots, N \quad (2)$$

An SLFN can approximate the NNN training samples with a mean error as expressed in (3), where a_i, b_i , and β_i denote the model parameters. Accordingly, the formulation can be expressed as in (4).

$$\sum_{i=1}^L \|o_j - t_j\| = 0 \quad (3)$$

$$\sum_{i=1}^L \beta_i G(a_i, b_i, x_j) = o_j, j = 1, \dots, N \quad (4)$$

In (4) can be further simplified as shown in (6)–(9). Here, H denotes the hidden layer output matrix of the SLFN. The i -th column of H corresponds to the output of the i -th hidden node associated with the input samples $x_1, x_2, x_3, \dots, x_N$. The hidden layer feature mapping is express using (5). Where $G(\cdot)$ represents the activation function. The i -th row of H corresponds to the feature mapping $h(x_i)$ of the input x_i . Furthermore, β denotes the output weight matrix, and T is the target output matrix of the ELM.

$$h(x) = G(a_1, b_1, x_N), \dots, G(a_L, b_L, x_N) \quad (5)$$

$$H \times \beta = T \quad (6)$$

$$H = \begin{bmatrix} h(x_1) \\ \vdots \\ h(x_N) \end{bmatrix} \quad (7)$$

$$H = \begin{bmatrix} G(a_1, b_1, x_1) & \dots & G(a_L, b_L, x_1) \\ \vdots & \dots & \vdots \\ G(a_1, b_1, x_N) & \dots & G(a_L, b_L, x_N) \end{bmatrix} \quad (8)$$

$$\beta = \begin{bmatrix} \beta_1^T \\ \vdots \\ \beta_L^T \end{bmatrix} \text{ and } T = \begin{bmatrix} T_1^T \\ \vdots \\ T_L^T \end{bmatrix} \quad (9)$$

In ELM, the input weights and hidden biases are randomly assigned. Consequently, the output weights associated with the hidden layer can be formulated as in (10).

$$\beta = H^T \times T \quad (10)$$

3. RESULTS AND DISCUSSION

The two-area power system, commonly referred to as the Kundur two-area test system, is illustrated in Figure 3. This benchmark network comprises four synchronous generators, two load centers, and eleven buses. Area 1 includes Generator 1, Generator 2, and Load 1, while Area 2 consists of Generator 3, Generator 4, and Load 2. The overall generation capacity of the system is 2819 MW, serving a total demand of 2734 MW. In Area 1, an inverter-based generation unit is incorporated, where its level of penetration is modeled by decreasing the effective inertia of the area in proportion to the increase in inverter capacity.

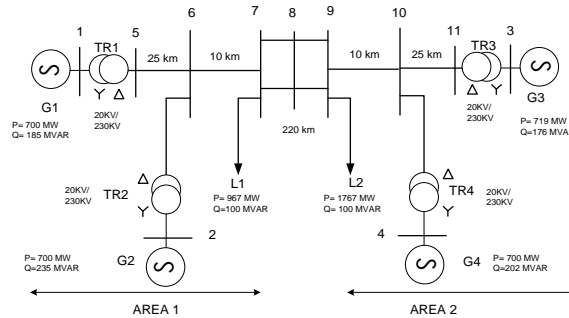


Figure 3. Two-area power system single line diagram

The first step focuses on showing the optimized parameter of virtual rotor control using BA. The parameters that have been optimized by BA are virtual damping gain and virtual inertia gain. There are eighteen different operating conditions in this paper. The VRC is optimized with BA for each operating condition. Table 1 shows the optimized VRC parameter in each operating condition. Variation of load and total inertia of Area 1 is considered as the fluctuations of the operating condition. The load is varied from 0.01-0.09 of the total generating capacity in Area 1. The inertia is varied from 100 to 50% of the total inertia from Area 1.

Table 1. Optimized parameter of VRC

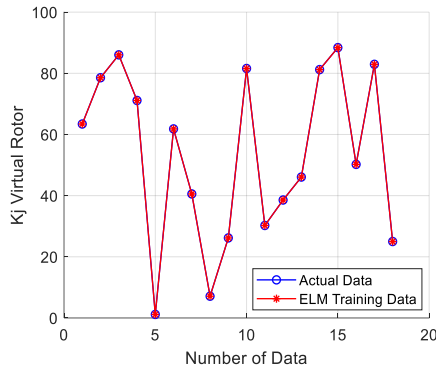
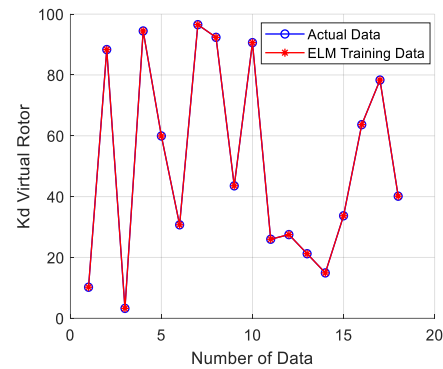
Load variation (pu)	Inertia variation (%)	K_j	K_d
0.01	100	63.4197	10.2053
	50	78.5501	88.3423
0.02	100	86.0295	3.2491
	50	71.1091	94.4610
0.03	100	1.1578	59.9316
	50	61.8158	30.7237
0.04	100	40.5493	96.5366
	50	7.1158	92.3641
0.05	100	26.1761	43.5434
	50	81.5650	90.6263
0.06	100	30.2469	25.9829
	50	38.5657	27.5096
0.07	100	46.0777	21.2204
	50	81.2050	14.9104
0.08	100	88.3938	33.6988
	50	50.2154	63.6629
0.09	100	82.9292	78.3242
	50	24.9958	40.1394

The variation of total system inertia is introduced to emulate the impact of integrating inverter-based generation. As presented in Table 1, the values of virtual damping and inertia gain differ across various operating conditions. These parameters are subsequently trained using the ELM, enabling the VRC to adapt to fluctuations in system operation. Through this approach, the transmission system operator (TSO) is relieved from the need to repeatedly optimize VRC parameters whenever operating conditions change.

At this stage, the performance of ELM in training VRC-optimized parameters is evaluated using the dataset summarized in Table 2. The inputs to the ELM are the variations in load and total inertia, while the outputs correspond to the VRC parameters. Figure 4 compares the values of K_j obtained from the BA with those predicted by ELM, while Figure 5 presents a similar comparison for K_d . The results clearly indicate that ELM is capable of accurately replicating the VRC parameters optimized by BA.

Table 2. Execution time comparison

Remarks	Duration (sec)
PSO	360
DEA	600
ELM	0.0033

Figure 4. Comparison between K_j obtained from the BA and K_j predicted by the ELMFigure 5. Comparison between K_d obtained from the BA and K_d predicted by the ELM

The ELM demonstrates high computational efficiency, requiring only 0.0033 seconds to obtain trained parameters. As shown in Figure 5, the error performance of K_j includes a maximum error of 0.0098, a minimum error of 0.0023, and a mean square error (MSE) of 0.005639, while for K_d , Figure 6 indicates a maximum error of 0.0069, a minimum error of 0.0022, and an MSE of 0.00525. These results confirm that ELM achieves both high prediction accuracy and strong generalization capability in estimating PI controller parameters.

In the testing phase, the trained VRC was evaluated under a 0.05 load change and a 50% reduction in total inertia in Area 1, considering two scenarios: VRC based on the BA (VRC-BA) and VRC based on ELM (proposed method). The dynamic frequency responses in Figure 6 show that both methods produce similar behavior, demonstrating that ELM can emulate BA-based VRC performance. However, the VRC-ELM system provides a smaller frequency nadir, indicating enhanced stability, while the frequency overshoot remains within ± 0.42 Hz, ensuring continuous operation without under-frequency or over-frequency violations. Overall, these findings demonstrate that VRC-ELM offers faster computation, accurate parameter estimation, and improved frequency stability compared to VRC-BA, suggesting its promise for applications in low-inertia power systems with high renewable penetration.

To evaluate the superiority of the proposed method, a comparison with existing approaches was conducted. The simulation considered a 0.05 load change in Area 1 along with a 50% reduction in total inertia to represent inverter-based power plant integration. As illustrated in Figure 7, the time-domain response of frequency deviations demonstrates that the system with VRC based on ELM achieves the best performance among the tested scenarios.

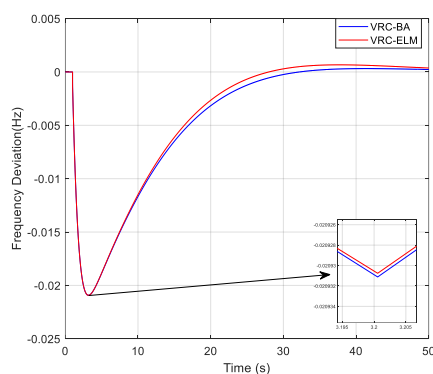


Figure 6. Dynamic response of frequency area 1 under different scenarios

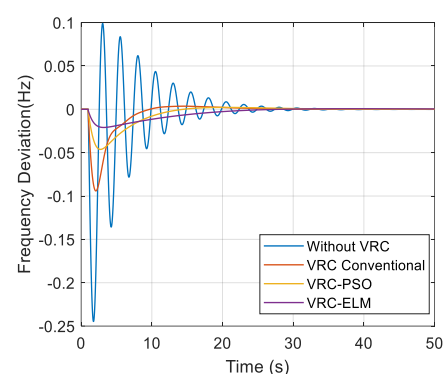


Figure 7. Comparison of time domain simulation in frequency area 1

In addition to dynamic performance, computational efficiency was assessed by comparing execution times with other well-known optimization methods, namely the differential evolution algorithm (DEA) and particle swarm optimization (PSO). As presented in Table 2, the proposed method achieves significantly shorter execution times than DEA and PSO, while maintaining comparable or superior accuracy. Although execution time is expected to increase with system size and complexity, the results highlight a favorable trade-off: the proposed ELM-based approach delivers faster computation without sacrificing performance, making it highly suitable for practical implementation in modern power systems.

To further demonstrate the efficacy of the ELM algorithm, a performance matrix is presented. Figure 8 illustrates the comparative performance of each algorithm under consideration. In this analysis, two key parameters frequency nadir and execution time are utilized to evaluate the overall performance and efficiency of the algorithms. These parameters are critical in assessing both the dynamic response and computational feasibility, particularly for real-time applications.

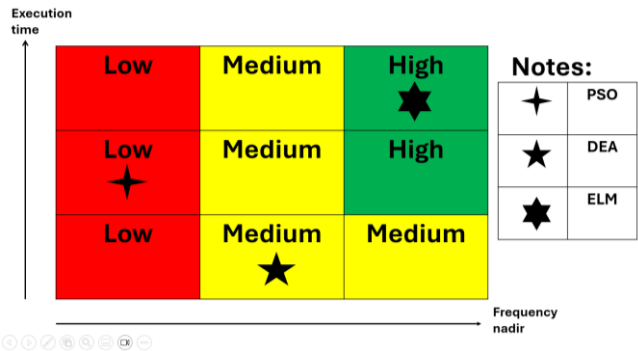


Figure 8. Performance matrix of each algorithm

As depicted in Figure 8, the ELM algorithm consistently outperforms both PSO and DEA across the selected metrics. Specifically, ELM achieves a lower frequency nadir, indicating a more stable dynamic response, and demonstrates significantly faster execution time, highlighting its suitability for time-sensitive applications. These results clearly support the conclusion that ELM offers a superior balance between control performance and computational efficiency compared to the other two algorithms.

4. CONCLUSION

This work introduces an intelligent VRC that integrates the BA for parameter optimization with the ELM for adaptive control, targeting enhanced frequency stability in power systems with high penetration of inverter-based renewable energy. Simulations conducted on a modified two-area test system demonstrate that the proposed controller adapts effectively to variations in both load and system inertia. Across 18 operating scenarios, the ELM was able to accurately replicate BA-optimized parameters with negligible prediction error, thereby ensuring consistent performance without the need for repeated re-optimization.

Dynamic performance evaluations further reveal that the ELM-based controller achieves superior frequency nadir and overshoot responses compared to BA-only and conventional methods, maintaining system stability under disturbances such as load fluctuations and inertia reduction. Moreover, the proposed approach exhibits a significant computational advantage, requiring only 0.0033 seconds, in contrast to 360 seconds for PSO and 600 seconds for DEA, making it well-suited for real-time applications. These results establish the method as a fast, accurate, and robust solution for frequency regulation in low-inertia grids. Future work may extend this study by incorporating RESs with uncertain outputs to further assess the robustness of the proposed framework.

FUNDING INFORMATION

The third author was supported by a Fundamental Research Grant administered by the Ministry of Education, Culture, Research, and Technology (Grant No. 074/UPER-WRP.1/PJN/VI/2025). The first authors is also very grateful to Telkom University for paying the article processing charging (APC) of this paper.

AUTHOR CONTRIBUTIONS STATEMENT

This journal uses the Contributor Roles Taxonomy (CRediT) to recognize individual author contributions, reduce authorship disputes, and facilitate collaboration.

Name of Author	C	M	So	Va	Fo	I	R	D	O	E	Vi	Su	P	Fu
Herlambang Setiadi	✓	✓	✓	✓	✓	✓	✓	✓	✓	✓	✓			✓
Baity Nuris Syifa		✓				✓		✓		✓				
Muhammad Abdillah	✓		✓	✓			✓			✓				
Yusrizal Afif						✓			✓	✓	✓			

C : Conceptualization

M : Methodology

So : Software

Va : Validation

Fo : Formal analysis

I : Investigation

R : Resources

D : Data Curation

O : Writing - Original Draft

E : Writing - Review & Editing

Vi : Visualization

Su : Supervision

P : Project administration

Fu : Funding acquisition

CONFLICT OF INTEREST STATEMENT

Authors state no conflict of interest.

DATA AVAILABILITY

Data availability is not applicable to this paper as no new data were created or analyzed in this study.




REFERENCES

- [1] H. Setiadi, D. A. Asfani, T. H. Nasution, M. Abdillah, and A. U. Krismanto, "Intelligent SMES based on Flower Pollination Algorithm on Wind Power System for Dynamic Stability Enhancement," *International Journal of Intelligent Engineering and Systems*, vol. 15, no. 1, pp. 341–349, 2022, doi: 10.22266/IJIES2022.0228.31.
- [2] H. Setiadi *et al.*, "Multi-Mode Damping Control Approach for the Optimal Resilience of Renewable-Rich Power Systems," *Energies*, vol. 15, no. 9, pp. 1–20, 2022, doi: 10.3390/en15092972.
- [3] O. Gonzales-Zurita, O. L. Andino, J. M. Clairand, and G. Escriva-Escriva, "PSO Tuning of a Second-Order Sliding-Mode Controller for Adjusting Active Standard Power Levels for Smart Inverter Applications," *IEEE Transactions on Smart Grid*, vol. 14, no. 6, pp. 4182–4193, 2023, doi: 10.1109/TSG.2023.3254908.
- [4] H. Setiadi, N. Mithulananthan, A. U. Krismanto, and I. Kamwa, "Optimization based design of dual input pss for improving small signal stability of power system with RESs," *International Journal on Electrical Engineering and Informatics*, vol. 11, no. 4, pp. 778–795, 2019, doi: 10.15676/ijeei.2019.11.4.10.
- [5] K. Arora, A. Kumar, V. K. Kamboj, D. Prashar, B. Shrestha, and G. P. Joshi, "Impact of renewable energy sources into multi area multi-source load frequency control of interrelated power system," *Mathematics*, vol. 9, no. 2, pp. 1–21, 2021, doi: 10.3390/math9020186.
- [6] M. A. Sobhy, A. Y. Abdelaziz, H. M. Hasanien, and M. Ezzat, "Marine predators algorithm for load frequency control of modern interconnected power systems including renewable energy sources and energy storage units," *Ain Shams Engineering Journal*, vol. 12, no. 4, pp. 3843–3857, 2021, doi: 10.1016/j.asej.2021.04.031.
- [7] D. H. Tungadio and Y. Sun, "Load frequency controllers considering renewable energy integration in power system," *Energy Reports*, vol. 5, pp. 436–453, 2019, doi: 10.1016/j.egy.2019.04.003.
- [8] M. Khasanov, S. Kamel, C. Rahmann, H. M. Hasanien, and A. Al-Durra, "Optimal distributed generation and battery energy storage units integration in distribution systems considering power generation uncertainty," *IET Generation, Transmission and Distribution*, vol. 15, no. 24, pp. 3400–3422, 2021, doi: 10.1049/gtd2.12230.
- [9] Y. Chi, Y. Xu, and R. Zhang, "Many-objective robust optimization for dynamic VAR planning to enhance voltage stability of a wind-energy power system," *IEEE Transactions on Power Delivery*, vol. 36, no. 1, pp. 30–42, 2021, doi: 10.1109/TPWRD.2020.2982471.
- [10] Z. Yue, Y. Liu, Y. Yu, and J. Zhao, "Probabilistic transient stability assessment of power system considering wind power uncertainties and correlations," *International Journal of Electrical Power & Energy Systems*, vol. 117, pp. 1–11, May 2020, doi: 10.1016/j.ijepes.2019.105649.
- [11] Y. Li *et al.*, "Coordinated Scheduling for Improving Uncertain Wind Power Adsorption in Electric Vehicles - Wind Integrated Power Systems by Multiobjective Optimization Approach," *IEEE Transactions on Industry Applications*, vol. 56, no. 3, pp. 2238–2250, 2020, doi: 10.1109/TIA.2020.2976909.
- [12] M. S. Javed, T. Ma, J. Jurasz, and M. Y. Amin, "Solar and wind power generation systems with pumped hydro storage: Review and future perspectives," *Renewable Energy*, vol. 148, pp. 176–192, 2020, doi: 10.1016/j.renene.2019.11.157.
- [13] J. Mitali, S. Dhinakaran, and A. A. Mohamad, "Energy storage systems: a review," *Energy Storage and Saving*, vol. 1, no. 3, pp. 166–216, 2022, doi: 10.1016/j.enss.2022.07.002.
- [14] S. Gurung, S. Naetiladdanon, and A. Sangswang, "Coordination of power-system stabilizers and battery energy-storage system controllers to improve probabilistic small-signal stability considering integration of renewable-energy resources," *Applied Sciences*, vol. 9, no. 6, pp. 1–22, 2019, doi: 10.3390/app9061109.
- [15] K. M. Kotb, M. F. Elmorshedy, H. S. Salama, and A. Dán, "Enriching the stability of solar/wind DC microgrids using battery and superconducting magnetic energy storage based fuzzy logic control," *Journal of Energy Storage*, vol. 45, pp. 1–24, Jan. 2022, doi: 10.1016/j.est.2022.103119.




- 10.1016/j.est.2021.103751.
- [16] S. Choudhury, "Review of energy storage system technologies integration to microgrid: Types, control strategies, issues, and future prospects," *Journal of Energy Storage*, vol. 48, p. 103966, 2022, doi: 10.1016/j.est.2022.103966.
 - [17] A. Naderipour, A. R. Ramtin, A. Abdullah, M. H. Marzbali, S. A. Nowdeh, and H. Kamyab, "Hybrid energy system optimization with battery storage for remote area application considering loss of energy probability and economic analysis," *Energy*, vol. 239, p. 122303, 2022, doi: 10.1016/j.energy.2021.122303.
 - [18] M. A. Shobug, N. A. Chowdhury, M. A. Hossain, M. J. Sanjari, J. Lu, and F. Yang, "Virtual Inertia Control for Power Electronics-Integrated Power Systems: Challenges and Prospects," *Energies*, vol. 17, no. 11, pp. 1–33, 2024, doi: 10.3390/en17112737.
 - [19] T. Kerdphol, F. S. Rahman, M. Watanabe, and Y. Mitani, "Robust Virtual Inertia Control of a Low Inertia Microgrid Considering Frequency Measurement Effects," *IEEE Access*, vol. 7, pp. 57550–57560, 2019, doi: 10.1109/ACCESS.2019.2913042.
 - [20] A. Saleh, W. A. Omran, H. M. Hasanien, M. Tostado-Véliz, A. Alkuhayli, and F. Jurado, "Manta Ray Foraging Optimization for the Virtual Inertia Control of Islanded Microgrids Including Renewable Energy Sources," *Sustainability*, vol. 14, no. 7, pp. 1–19, 2022, doi: 10.3390/su14074189.
 - [21] S. K. Singh, R. Singh, H. Ashfaq, and R. Kumar, "Virtual Inertia Emulation of Inverter Interfaced Distributed Generation (IIDG) for Dynamic Frequency Stability & Damping Enhancement Through BFOA Tuned Optimal Controller," *Arabian Journal for Science and Engineering*, vol. 47, no. 3, pp. 3293–3310, 2022, doi: 10.1007/s13369-021-06121-5.
 - [22] U. Markovic, O. Stanojev, P. Aristidou, E. Vrettos, D. Callaway, and G. Hug, "Understanding Small-Signal Stability of Low-Inertia Systems," *IEEE Transactions on Power Systems*, vol. 36, no. 5, pp. 3997–4017, Sep. 2021, doi: 10.1109/TPWRS.2021.3061434.
 - [23] M. Eskandari, A. V. Savkin, and J. Fletcher, "A Deep Reinforcement Learning-Based Intelligent Grid-Forming Inverter for Inertia Synthesis by Impedance Emulation," *IEEE Transactions on Power Systems*, vol. 38, no. 3, pp. 2978–2981, 2023, doi: 10.1109/TPWRS.2023.3242469.
 - [24] K. Singh and Zaheeruddin, "Enhancement of frequency regulation in tidal turbine power plant using virtual inertia from capacitive energy storage system," *Journal of Energy Storage*, vol. 35, pp. 1–16, 2021, doi: 10.1016/j.est.2021.102332.
 - [25] P. Lakshmi, B. V. Rao, R. Devarapalli, and P. Rai, "Optimal Power Flow with BAT algorithm for a Power System to reduce transmission line losses using SVC," in *2020 International Conference on Emerging Frontiers in Electrical and Electronic Technologies (ICEFEET)*, 2020, pp. 1–5, doi: 10.1109/ICEFEET49149.2020.9186964.
 - [26] T. Kerdphol, F. S. Rahman, M. Watanabe, and Y. Mitani, *Virtual Inertia Synthesis and Control*. in Power Systems, 1st ed. Cham: Springer International Publishing, 2021, doi: 10.1007/978-3-030-57961-6.
 - [27] S. Gurung, F. Jurado, S. Naetiladdanon, and A. Sangswang, "Comparative analysis of probabilistic and deterministic approach to tune the power system stabilizers using the directional Bat algorithm to improve system small-signal stability," *Electric Power Systems Research*, vol. 181, pp. 1–10, 2020, doi: 10.1016/j.epsr.2019.106176.
 - [28] H. Setiadi, N. Mithulananthan, R. Shah, K. Y. Lee, and A. U. Krismanto, "Resilient wide-area multi-mode controller design based on Bat algorithm for power systems with renewable power generation and battery energy storage systems," *IET Generation, Transmission and Distribution*, vol. 13, no. 10, pp. 1884–1894, 2019, doi: 10.1049/iet-gtd.2018.6384.
 - [29] I. Manuaba, M. Abdillah, R. Zamora, and H. Setiadi, "Adaptive Power System Stabilizer Using Kernel Extreme Learning Machine," *International Journal of Intelligent Engineering and Systems*, vol. 14, no. 3, pp. 468–480, 2021, doi: 10.22266/ijies2021.0630.39.
 - [30] B. Liu, G. Chen, H. C. Lin, W. Zhang, and J. Liu, "Prediction of IGBT junction temperature using improved cuckoo search-based extreme learning machine," *Microelectronics Reliability*, vol. 124, p. 114267, Sep. 2021, doi: 10.1016/j.microrel.2021.114267.

BIOGRAPHIES OF AUTHORS






Herlambang Setiadi    is Assistant Professor at School of Electrical Engineering, Telkom University. He received a bachelor degree from Institut Teknologi Sepuluh Nopember (Surabaya, Indonesia) majors in Power system Engineering in 2014. Then, master degree from Liverpool John Moores University (Liverpool, United Kingdom), majors in Electrical Power and Control Engineering in 2015. Furthermore, he received a Doctoral degree from The University of Queensland. Before joining Telkom University, he was investigator at INECS TEC Portugal and Lead Renewable Energy Engineering at Synkrona Enjiniring Nusantara. His research interests power system dynamic and control, renewable energy integration and metaheuristic algorithm. He can be contacted at email: herlambangsetiadi@telkomuniversity.ac.id.






Baity Nuris Syifa    was born in Surabaya, East Java, Indonesia in 2000. She received bachelor and engineering degree in electrical engineering from Institut Teknologi Sepuluh Nopember (ITS), Surabaya, Indonesia, in 2021. In 2023, She received a Master Engineering degree in electrical engineering from Institut Teknologi Sepuluh Nopember (ITS). She is currently a doctoral student in The University of Queensland. Her research focuses mainly on power system stability and smart grids. She can be contacted at email: b.syifa@uq.edu.au.



Muhammad Abdillah    was born in Pasuruan. He received Sarjana Teknik (equivalent to B.Eng.), and Magister Teknik (equivalent to M.Eng.) degrees from Department of Electrical Engineering, Institut Teknologi Sepuluh Nopember (ITS), Surabaya, Indonesia in 2009 and 2013, respectively. He obtained Dr Eng. degree from Graduate School of Engineering, Hiroshima University, Japan in 2017. He is currently working as a lecturer at the Department of Electrical Engineering, Universitas Pertamina, Jakarta, Indonesia. As author and co-author, he had published 100 scientific papers in different journals and conferences. He was a member of IEEJ, IAENG, and IEEE. His research interests are power system operation and control, power system optimization, robust power system security, power system stability, intelligent control and system, and artificial intelligence (optimization, machine learning, and deep learning). He can be contacted at email: m.abdillah@universitaspertamina.ac.id.



Yusrizal Afif    was born in Surabaya, East Java, Indonesia in 1992. He received Bachelor and Engineering degree in Electrical Engineering from Institut Teknologi Sepuluh Nopember, Surabaya, Indonesia, in 2015. From 2015 to 2017 he worked as electrical engineer at Krakatau Engineering Co., Indonesia. He received Master Engineering degree in Electrical Engineering from Institut Teknologi Sepuluh Nopember in 2019. He was joined Airlangga University in 2020 as lecturer. His research concentrates mainly on high voltage technology, apparatus characteristics, discharge phenomena, and renewable energy. He can be contacted at email: yusrizal@ftmm.unair.ac.id.